Materials Research Express

PAPER • **OPEN ACCESS**

Silicone elastomers filled with rare earth oxides

To cite this article: Mihail Iacob *et al* 2020 *Mater. Res. Express* **7** 035703

Materials Research Express

PAPER

Silicone elastomers filled with rare earth oxides

Mihail Iacob[1], **Anton Airinei**[1], **Mihai Asandulesa**[1], **Mihaela Dascalu**[1], **Nita Tudorachi**[1], **Leonor Hernandez**[2] **and Maria Cazacu**[1]

[1] 'Petru Poni' Institute of Macromolecular Chemistry, Grigore Ghica Voda Alley, 41A, 700487 Iasi, Romania
[2] Universitat Jaume I. Departamento de Ingenieria Mecanica y Construccion, Castellon de la Plana, 12071, Spain

E-mail: iacob.mihai@icmpp.ro

Keywords: silicone, rare earth oxides, active fillers, composites, hydrophobicity

Supplementary material for this article is available online

OPEN ACCESS

RECEIVED
30 October 2019

REVISED
14 February 2020

ACCEPTED FOR PUBLICATION
26 February 2020

PUBLISHED
9 March 2020

Abstract

Silicones which possess, amongst others, remarkable mechanical properties, thermal stability over a wide range of temperatures and processability, and rare earth oxides (REO), known for their unique optic, magnetic and catalytic properties can be coupled into multifunctional composite materials (S-REOs). In addition, the intrinsic hydrophobicity of REO and polysiloxanes makes them easily compatible without the need for surface treatments of the former. Thus, europium oxide (Eu_2O_3), gadolinium oxide (Gd_2O_3) and dysprosium oxide (Dy_2O_3) in amounts of 20 pph are incorporated as fillers into silicone matrices, followed by processing mixture as thin films and crosslinking at room temperature. The analysis of the obtained films reveals the changes induced by these fillers in the thermal, mechanical, dielectric and optical properties, as well as the hydrophobicity of the silicones. The luminescence properties of S-REO composites were investigated by fluorescence spectra and lifetime - resolved measurements with a multiemission peaks from blue to greenish register. The thermogravimetrical analysis indicates an increasing of thermal stability of the composites that contain REO, compared to pure silicone. As expected, the dielectric permittivity significantly increased due to nature of the fillers, while the dielectric loss values are relatively low for all samples, indicating a minimal conversion of electrical energy in the form of heat within bulk composites. The presence of rare earth oxides into the silicone matrix facilitates the motions of long-range charge carriers through the network resulting in higher values of conductivity of the composite films. The stress-strain measurements revealed the reinforcing effect of the rare earth metal oxides on a silicone matrix, leading to a significant increase of Young modulus. The known hydrophobicity of silicones is further enhanced by the presence of REO.

1. Introduction

The scientific and technological interest of rare earths is based on their special physical (optical, electrical, magnetic) or chemical (e.g., catalytic, anti-corrosive) properties that are caused by their particular electronic structure (4f orbitals with parallel-spin unpaired electrons, being paramagnetic) [1, 2]. The optical materials doped with rare earths are of interest for light sources in optoelectronics, for optical amplification and other elements of photonics [3]. Rare earths can extend the life of the free radicals, by rapidly catching electrons on orbital 4f [3]. X-ray shielding studies at different tube voltages, with polymer composites of different thicknesses, especially based on natural rubber incorporating varying amounts of modified rare earth oxides (REO), indicate the latter as promising materials for medical imaging [4]. The results of some researches also suggest the applicative potential of REO as additives to polymers for the attenuation of ionizing radiation [5]. REO are capable of absorbing strongly in the near-UV spectrum (300 nm), thus being useful in coating technologies as UV absorbers [6].

These materials are generally prohibitively expensive to be widely used due to resource poverty, some sources indicating a production of about 18,000 tons annually, of which about 85% are used in the production of

catalysts and glass manufacturing [5], although new technology trends are developing [7]. However, achieving the desired performance could justify their use, especially where there is a maximum benefit with low consumption of such materials.

Silicones, organic-inorganic materials mainly based on polydimethylsiloxanes are materials with high application potential thanks to special properties, such as uniform physical characteristics over a wide temperature range, resistance to weathering and ageing, good electrical properties, water repellency and, especially, environmental compatibility during manufacture and use, which makes them accepted by the wide public. They are used in almost all industry areas, thus being present in most of the things that we are using in our daily life [8]. The variety of silicone applicability domains, as well as the growing demands and exigencies in terms of performance, motivate the intensification of studies for the continuous upgrading of these materials. Among the approaches, along with those in principle consisting of chemical modification, a path that offers many design opportunities is the incorporation of suitable active fillers to induce or enhance certain properties. It is known that the incorporation of a small amount of REO into polymers induces significant improvements in their properties, such as thermal stability, conductivity, hydrophobicity, surface or texture properties, etc [9].

Several studies revealed the benefits of adding REOs to a polymer matrix. For example, poly(*o*-aminophenol) (POAP) containing Eu_2O_3 nanoparticles was found to have larger specific capacitance, lower charge-transfer resistance, higher density of active centres, better performance compared to pure POAP, thus being more efficient for application in supercapacitors [10]. Using of Eu_2O_3 as filler for urethane dimethacrylate (UDMA) based composites lead to increasing of fluorescence intensity, while the change in the composite colour was quite small. Clear fluorescence was observed when Dy_2O_3 and Tb_4O_7 were used as fillers for UDMA based composites [11]. Incorporation of Eu_2O_3 into polypyrrole/CuO results in increasing of their capacitive performances [12]. In another study, it was demonstrated that adding Dy2O3 to the polyetheretherketone based composites increase their x-ray shielding properties [13]. REOs were used as flame retardants for thermoplastic polyolefins based on polypropylene/poly(octylene-co-ethylene) blends [14] or Nylon 1010/ethylene-vinyl-acetate rubber thermoplastic elastomers [15]. Polymers with REO nanocrystals are indicated to be useful for luminescent solar concentrators [16]. It is reported that an addition of 1 wt% CeO_2 to polypropylene increases its resistance to photodegradation, as well as its thermal stability [2, 6]. In fact, REOs have been used as thermal stabilizers for PVC since the 1990s [7]. Sm_2O_3 was used as cocatalyst and nucleating agent in the reactive extrusion of cardanol-grafted polypropylene to improve the mechanical properties and processability [2]. CeO_2 proved to be an efficient reinforcing agent for natural rubber [17]. As additives to silicones, generally, in studies reported in literature [9, 18], REO have been used together with silica (Ceria/Silica [9] or Ceria–Zirconia–Silica@PDMS [18]). There is a report in 1974 [19] about the thermostabilizing effect of rare-earth metal oxides on methylvinylsilicone rubbers.

In the context of our preoccupations for the improvement of silicone performance for specific applications, especially as active elements in electromechanical devices, different fillers: organic (polyazometines) [20], inorganic (iron oxides [21, 22], silver [23, 24], barium titanate, [25, 26] titanium dioxide [27, 28],), organic-inorganic (organosilesquioxanes [29, 30]), etc were incorporated in silicone derivatives. In this paper, the effect of three REOs (Eu_2O_3, Gd_2O_3 and Dy_2O_3) as single fillers on the silicone behaviour was studied. The intrinsic hydrophobicity of REO and polysiloxanes creates the premises for better compatibility, without the need for additional actions for this [31]. To simplify the study, we used the same polymeric matrix based on a PDMS of molecular weight $M = 60{,}000\ g\ mol^{-1}$ cross-linked by condensation with TEOS, and the REO were incorporated in the same percentage (20 pph) in all cases. Mechanical, dielectric, thermal, photoluminescent propertie, as well as moisture behaviour of the resulted composites, have been studied in comparison to the simple matrix considered as a reference in order to evaluate the effects of rare earth oxide addition on silicones. While the thermal degradation pattern of simple polysiloxane systems is relatively well studied and understood, the identification of chemical reactions occurring during the decomposition of polymers filled with nanoparticles is more complicated [9]. Therefore, the pyrolysis products of PDMS- REO composites prepared in this work were studied by TGA coupled with FTIR.

2. Experimental

2.1. Materials

Polydimethylsiloxane-α,ω-diol (PDMS) of molecular mass $M_n = 60{,}000\ g{\cdot}mol^{-1}$ (determined by GPC in chloroform) was synthesized by cationic ring-opening polymerization following the procedure described in reference [32]. Eu_2O_3, Gd_2O_3 or Dy_2O_3 (commercial reagents) were ultrasonicated in toluene for 5 min before adding to the composite reaction mixture. Dibutyltin dilaurate (DBTDL), tetraethoxysilane (TEOS) and toluene were high-purity reagents purchased from Sigma-Aldrich.

2.2. Methods

The morphology of the prepared nanocomposites films was studied using a scanning electron microscope (SEM, Quanta 200) in cryo-fractured section. The SEM is operating at 20 kV with secondary and backscattering electrons in low-vacuum mode. Thermal degradation of polydimethylsiloxane (PDMS) thin films containing rare earth metal oxides and evolved gas analysis were performed using a TG-DTA/FTIR system. The system was equipped with a thermobalance model STA 449 F1 Jupiter (Netzsch-Germany) and a FTIR spectrophotometer, model Vertex-70 (Bruker-Germany). The sample weight varied from 10 to 15 mg. The samples were scanned from 30 °C to 650 °C, at a heating rate of 10 °C min^{-1} and a nitrogen gas flow rate of 40 ml min^{-1}. The samples were heated in open aluminium crucibles and an aluminium crucible as reference material was utilized. The evolved gases were transferred in a TGA-IR external modulus of the spectrometer. The infrared absorption spectra were recorded over the wavenumber range of 600–4000 cm^{-1} with a resolution of 4 cm^{-1}. TGA-IR modulus contains a low volume gas cell (V = 8.7 ml) of 123 mm length and it was heated at 190°C to avoid the condensation of the gaseous compounds. The acquisition of FTIR spectra in 3D size was carried out with OPUS 6.5 software. Dielectric permittivity analyses were carried out with a broadband dielectric spectrometer (Novocontrol Technologies, Germany) equipped with an Alpha-A high performance frequency analyzer. The film nanocomposites are sandwiched between two cylindrical gold coated plate electrodes as a sandwich capacitor and further integrated into the BDS1200 standard sample cell. Mechanical tests were performed on dumbbell-shaped cut samples from thin films on a TIRA test 2161 apparatus, Maschinenbau GmbH Ravenstein, Germany. Measurements were run at an extension rate of 20 mm min^{-1}, at ambient temperature. Fluorescence spectra of thin films were obtained on a Perkin Elmer LS55 luminescence spectrometer with a xenon lamp as the light source. Fluorescence lifetimes measurements were performed with an Edinburgh Instruments FSL 980 photoluminescence spectrometer using time-correlated single photon counting technique. A microsecond lamp was used as an excitation source. Decay data analysis was made using a deconvolution procedure with a multiexponential decay model. The quality of the data fits was evaluated by chi-squared (χ^2) parameter. Water vapour sorption capacity of the samples have been measured in dynamic regime by using the fully automated gravimetric analyzer IGAsorp produced by Hiden Analytical, Warrington (UK).

2.3. Preparation of PDMS—rare earth oxide composites

PDMS-rare earth oxide composites were prepared by the following procedure: 0.75 g of polydimethylsiloxane-α,ω-diol (M_n = 60,000 g·mol^{-1}) were dissolved in 10 ml of toluene and mixed with 0.15 g (20 pph, parts per hundred) of Eu_2O_3, Gd_2O_3 or Dy_2O_3 in order to prepare composites S-Eu_2O_3, S-Gd_2O_3 or S-Dy_2O_3, respectively. The reaction mixture was stirred for 15 min using magnetic stirring and then mixed with 0.07 ml of TEOS (crosslinking agent) and stirred for 30 min, followed by adding 10 μl of DBTDL (catalyst). After another 5 min of stirring, the reaction mixture was poured as a film on a Teflon substrate using Dr Blade and aged for about two weeks in the laboratory environment. The reference sample prepared without the addition of rare earth oxide and encoded as PDMS.

2.4. Results and discussion

A series of silicone-rare earth oxide (S-REO) composites were prepared by physical mixing in bulk and stabilized by room temperature vulcanization. Firstly, the components were mixed under magnetic stirring. Polydimethylsiloxane-α,ω-diol (M_n = 60,000 g·mol^{-1}) was used as the polymeric matrix, REOs as fillers, toluene as solvent, tetraethyl orthosilicate as a crosslinker and dibutyltin dilaurate as a catalyst. Further, the reaction mixture was poured onto a Teflon substrate and left for two weeks in order for crosslinking and ageing. The prepared composites were labelled as S-Eu_2O_3, S-Gd_2O_3 and S-Dy_2O_3 for the composites containing 20 pph of Eu_2O_3, Gd_2O_3 and Dy_2O_3 respectively, while the reference sample without filler is designated PDMS.

The morphology of the prepared film composites was studied using SEM in cryo-fractured section (figure 1). In order to avoid the migration of siloxane polymer chains to the surface of composite material, the samples were frozen in liquid nitrogen and immediately fractured before analysing. Compared to the reference sample, it can be observed that in all composites the REO filler is uniformly dispersed in the polymer matrix as micrometres sized agglomerates.

The thermal stability of unfilled silicone (PDMS) and their composites containing REOs (Eu_2O_3, Gd_2O_3 and Dy_2O_3) was investigated by thermogravimetric analysis coupled with FTIR under inert atmosphere (nitrogen). The thermal decomposition behaviour of PDMS - REO composites at a heating rate of 10 °C min^{-1} are shown graphically in figure 2 in terms of TG and DTG curves, while the main parameter extracted from them are summarized in table 1.

The TG curve of PDMS shows two stages of degradation. The first decomposition stage occurs between 220 and 360 °C with an onset temperature of 283 °C, a weight loss of 11.63% and a degradation rate of 1.87%/min. The second stage span over 360 °C–580 °C and the corresponding weight loss was 81.15% with a much higher

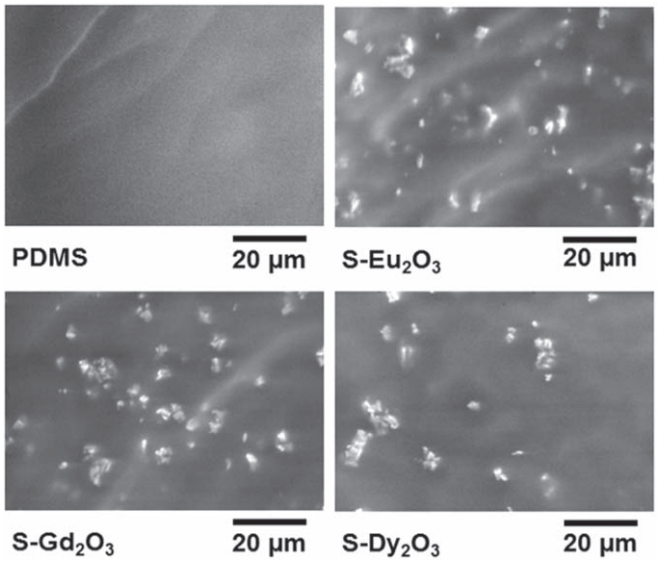

Figure 1. SEM images of composites.

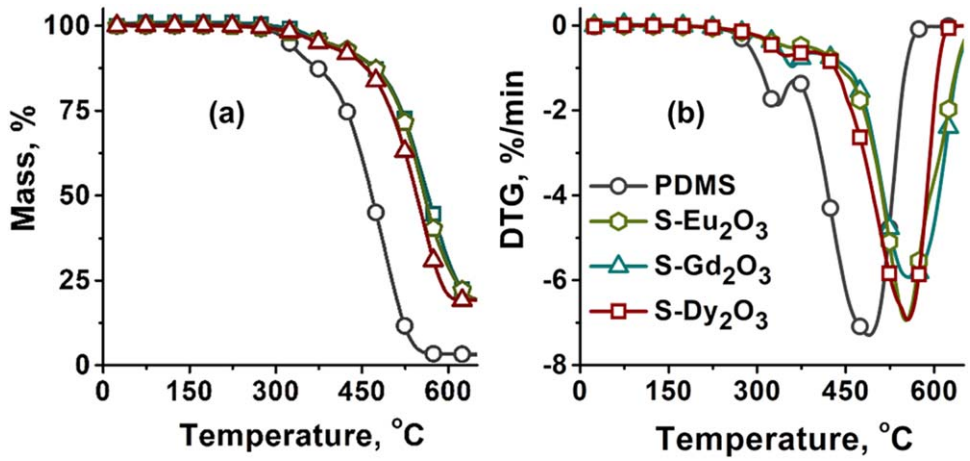

Figure 2. TGA (a) and DTG curves (b) of crosslinked PDMS and PDMS-REO composites.

degradation rate of 7.30%/min. The thermal degradation of PDMS-REO composites takes place in two ($S\text{-}Gd_2O_3$, $S\text{-}Dy_2O_3$) or three ($S\text{-}Eu_2O_3$) stages with a minor weight loss, between 4.83 and 5.95%, in the first stage.

The temperature corresponding to 10% weight loss (T_{10}) was considered as a criterion for thermal stability of metal composites. The 10% weight loss temperatures were over 440 °C as compared with 335 °C for PDMS suggesting that the incorporation of REOs in PDMS matrix results in composites with increased thermal stability as compared with unfilled silicone. The hierarchy of samples, according to their thermal stability, is the following: PDMS $<$ $S\text{-}Dy_2O_3$ $<$ $S\text{-}Gd_2O_3$ $<$ $S\text{-}Eu_2O_3$. Also, an inspection on DTG data (figure 2(b)) showed that the maximum degradation temperature (T_{max}) was found out at much higher temperatures, over 550 °C, for S-REO as compared to PDMS reference.

The increase of the temperature over 360 °C leads to major degradation of the S-REO samples occurring the breaking of some C-Si and Si-O bonds from PDMS matrix and the formation of some cyclic oligosiloxanes with a low polymerization degree, between 3 and 12 [33, 34]. Compared to the degradation pattern of PDMS or $S\text{-}Gd_2O_3$ and $S\text{-}Dy_2O_3$, the degradation of $S\text{-}Eu_2O_3$ involves a second process ranged between 358 and 552 °C with a corresponding weight loss of up to 19.31% (table 1). In this stage, the formation and elimination of some cyclosiloxane oligomers having low molecular weight can occur. Major degradation stage spans over 450 and 520 °C depending on the rare earth metal nature. The weight losses in the main degradation process are higher and varied between 70.97 and 75.02%. The increase of the temperature up to 650 °C determines the breaking of

Table 1. Summary of thermal data for PDMS and PDMS-REO composites.

Sample	Degradation stage	T_{onset} °C	T_{max} DTG °C	W wt%	T_{10} °C	T_{20} °C	R (700 °C) (%)
PDMS	I	283	335	11.63	353	410	3.22
	II	391	489	85.15			
S-Gd_2O_3	I	327	361	5.95	452	507	19.03
	II	476	553	75.02			
S-Eu_2O_3	I	272	358	4.83	453	503	19.31
	II	417	451	4.89			
	III	480	552	70.97			
S-Dy_2O_3	I	302	350	5.91	442	487	19.11
	II	448	555	74.98			

T_{onset} - the temperature at which the thermal degradation begins.
T_{max}- the temperature of maximum decomposition rate.
T_{10}- temperature corresponding to 10% weight loss.
T_{20}- temperature corresponding to 20% weight loss.
W- weight loss.
R- residual weight at 700 °C.

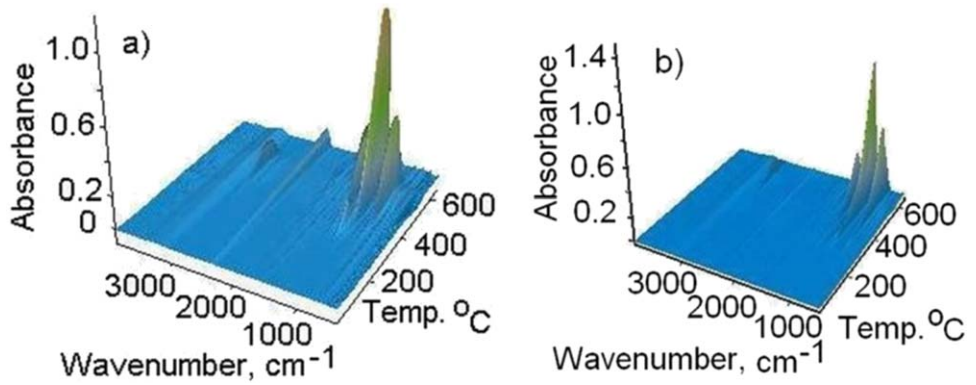

Figure 3. 3D-FTIR spectra of PDMS (a) and PDMS-Eu_2O_3 (b) thin films.

C-Si and Si-O bonds leading to the PDMS depolymerization as well as to the splitting of cyclosiloxane oligomers with higher molecular weights.

The metal oxide content can be determined by thermogravimetric analysis. The residue at 650 °C can be estimated by the difference between the residue of S-REO composite (table 1) and char yield of PDMS (3.22%). The residue values of metal oxide in S-REO composites are as follows: S-Gd_2O_3: 15.81%; S-Dy_2O_3: 16.09%; S-Eu_2O_3: 15.89%.

The composition of gaseous products in the thermal degradation of S-REO composites was analysed by FTIR absorption spectroscopy. The evolved gases were monitored for PDMS and S-Eu_2O_3 composite because all the polymer films exhibit the same degradation pattern. The 3D-FTIR spectra of PDMS and S-Eu_2O_3 thin films are illustrated in figure 3. The FTIR spectra exhibited practically the same evolution as a function of temperature since only the polymer matrix undergoes the thermal degradation. The presence of evolved gases was remarked after 350 °C–400 °C when the degradation process begins according to TG/DTG diagrams.

In figure S1 is available online at stacks.iop.org/MRX/7/035703/mmedia, the FTIR spectra corresponding to temperatures close to DTG peaks are depicted for PDMS (335 °C) and S-Eu_2O_3 composite (358 °C). The characteristic absorption bands at about 3587–3980 cm^{-1} and 1419–1791 cm^{-1} are due to νOH vibrations, while those at 2342, 2360 cm^{-1} are assigned to evolved CO_2. The profiles of the IR absorption spectra of S-Me_2O_3 composites at different degradation temperatures are practically similar (figure S1), water, methane, carbon dioxide being the main decomposition products. Thus, the absorption bands located at 2896, 2970 cm^{-1} are specific to asymmetric CH stretching vibrations in CH_3 groups and methane, arising in the thermal degradation of PDMS. The strong absorption bands at 1028 and 1068 cm^{-1} can be provided by Si-O-Si stretching vibrations. The absorption bands around 1265 cm^{-1} and 816 cm^{-1} can be assigned to CH_3 deformation vibration in Si-CH_3 and to the Si-C stretching vibrations in Si-CH_3 [34, 35]

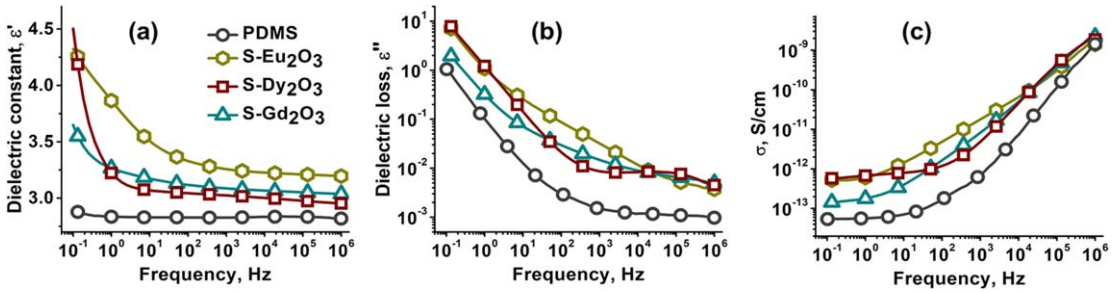

Figure 4. Dielectric properties for S-REO composites: dielectric constant (a), dielectric loss (b) and conductivity values as a function of frequency (c).

Table 2. Dielectric data of the prepared composites.

Sample	ε'		ε''		Conductivity, S•cm^{-1}	
	0.1 Hz	10^3 Hz	0.1 Hz	10^3 Hz	0.1 Hz	10^3 Hz
PDMS	2.9	2.8	1.07	$1.5{\cdot}10^{-3}$	$5.4{\cdot}10^{-14}$	$6.8{\cdot}10^{-13}$
S-Eu_2O_3	4.3	3.3	9.6	$3.2{\cdot}10^{-2}$	$5.3{\cdot}10^{-13}$	$1.8{\cdot}10^{-11}$
S-Gd_2O_3	3.7	3.1	2.5	$1.5{\cdot}10^{-2}$	$1.4{\cdot}10^{-13}$	$8.2{\cdot}10^{-12}$
S-Dy_2O_3	4.5	3.0	10.3	$8.7{\cdot}10^{-3}$	$5.7{\cdot}10^{-13}$	$4.8{\cdot}10^{-12}$

The principles of dielectric spectroscopy are widely used to gain insight into the storage and dissipation of energy in a variety of different materials. The dielectric dispersion is achieved by placing a material in contact with two electrodes and applying an alternating electric field over a broad range of frequency. In this study, the dielectric response, in terms of dielectric constant (ε') and dielectric loss (ε'') parameters, was recorded at room temperature, within 0.1 Hz 1.0 MHz electric field frequency range in order to evaluate the influence of some REOs on the dielectric behaviour of a polymeric matrix based on PDMS. The conductivity of charge carriers (σ) was further estimated from the dielectric loss with the relation:

$$\sigma = 2\pi\varepsilon_0 f\varepsilon'' \quad (1)$$

where ε_0 is the permittivity of free space and f is the frequency of the alternating electric field [36].

As generally known, the dielectric constant is related to the ability of dipoles to orient in the direction of an applied alternative field [37]. It depends, thus, by the frequency of the alternating field and can follow the chemical changes in analysed materials. The evolution of dielectric constant, dielectric loss and conductivity of the S-REO composites as a function of frequency are presented in figure 4 and table 2. According to figure 4(a), ε' value decreases gradually towards increasing frequency since the polarizable units need a longer time than the oscillations of the applied alternative field. According to literature, the intensive decline of ε' within the low frequency region might be caused by an electrode polarization-type effect [38, 39]. However, the decline seems to be more pronounced for S-REO composites, as compared with that of the reference sample, revealing an intense dipolar activity. The electrode polarization is an effect of charges accumulation at the electrodes and overlaps with the dipolar-type signal. At higher frequencies, the electrode-polarization-type signal is reduced and the intrinsic dipolar activity of the samples is revealed.

The dielectric constant values retrieved in the electrode polarization region (0.1 Hz) and the 'real' dipolar activity region (10^3 Hz) are presented in table 2. The lowest values of ε' are retrieved for PDMS reference, being comparable with other silicone composites, e.g. containing TiO_2 nanoparticles that provide dielectric constants between 2.97 and 4.4 [40]. An increase of ε' (for f = 10^3 Hz, from ε'(PDMS) = 2.8 to ε'(S-Eu_2O_3) = 3.3) is furnished by composite materials, due to the high dielectric constant of REOs.

The dielectric loss is correlated to the dissipation of electromagnetic energy, required for molecular motions and present a similar behaviour with frequency as dielectric constant (figure 4(b)). It can be seen that the dielectric loss values are relatively low in the whole frequency range, indicating a minimal conversion of electrical energy in the form of heat within bulk composites. Considering conductivity data (figure 4(c)), it can be deduced that all the materials analysed are electrical insulators. Moreover, the σ(f) dependences exhibit two different regimes: at low frequencies, the conductivity is related to long-range electrical charges of direct current conductivity (σ_{dc}), while at high frequencies, the conductivity signal is attributed only to bound charges of the alternating current conductivity (σ_{ac}). In other words, the movements of charge carriers are retrieved from the

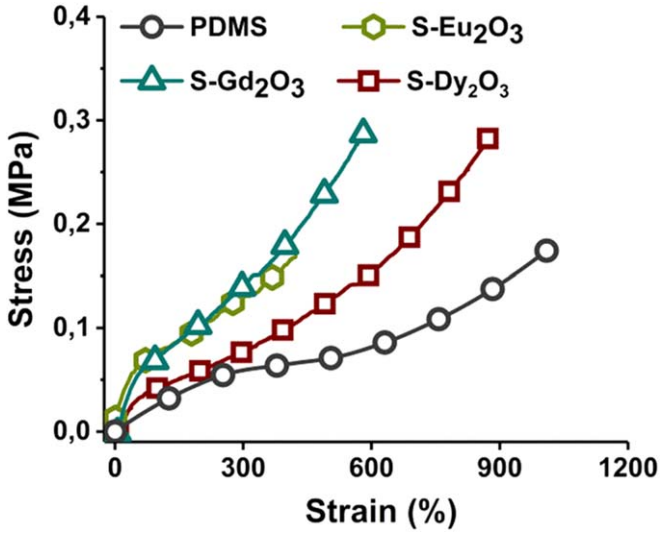

Figure 5. Stress-strain curves for S-PDMS composites.

Table 3. Mechanical parameters estimated on the basis of stress-strain curves.

Sample	Strain at break, ε, %	Stress at break, σ, MPa	Young modulus,[a] MPa
PDMS	1020	0.18	0.035
S-Eu_2O_3	422	0.17	0.28
S-Gd_2O_3	580	0.29	0.14
S-Dy_2O_3	874	0.29	0.09

[a] Young's modulus calculated at 10% strain.

frequency-independent plateau of σ_{dc}, and the dipolar behaviour is displayed on the linear increase of conductivity with the frequency. On the other hand, the higher values of conductivity for composite films reveal that the presence of REOs facilitates the motions of long-range charge carriers through the network.

The mechanical properties of the S-REO composites were studied based on stress-strain curves (figure 5, table 3). As can be seen, all samples show nonlinear behaviour in stress-strain relation, of sigmoidal type, characteristic for highly deformable elastomers [41, 42], similar with those obtained by Carpi *et al* on silicones having dispersed 10 vol% lead magnesium niobate–lead titanate (PMN–PT) [43]. As expected, REO filler has a reinforcing effect on silicone matrix, leading to increasing of Young modulus from 0.035 MPa for pure silicone to 0.28, 0.14 and 0.09 for S-Eu_2O_3, S-Gd_2O_3 and S-Dy_2O_3 respectively. As the polarity increases from europium oxide to dysprosium oxide, their compatibility with the silicone matrix and consequently the strengthening effect decrease in the same order.

Although composites are stiffer compared to pure PDMS, Young's modulus remains low for all analyzed samples. Strain at break is 1020, 420, 580 and 874% for PDMS, S-Eu_2O_3, S-Gd_2O_3 and S-Dy_2O_3 respectively.

The rare earth metals such as Eu, Dy, Nd are visible luminescence centres and their incorporation into a host matrix can open some channels for efficient visible light emission [44]. The emission spectra of metal oxide/REO films excited at 280 nm are shown in figure 6(a). The emission spectra of prepared composites present practically very similar profiles with dominating emission bands located around 420, 460, 480 and 520 nm, respectively. As can be verified, the intensity of the emission bands was affected by the employed excitation wavelength, suggesting that the energy transfer process was influenced by the siloxane matrix. The highest intensity of the emission was obtained for excitation at 280 nm, while for other wavelengths the fluorescence intensity decreases as the excitation energy decreases (figure 6(b)). Also, the shape and the position of the emission bands are not dependent on the excitation energy, they are mainly influenced by the nature of rare earth metal. This means that the effect of the local rare earth metal surrounding distribution is practically negligible indicating a good dispersion of the emission centres in the polymer matrix, as it seems from the SEM images (figure 1).

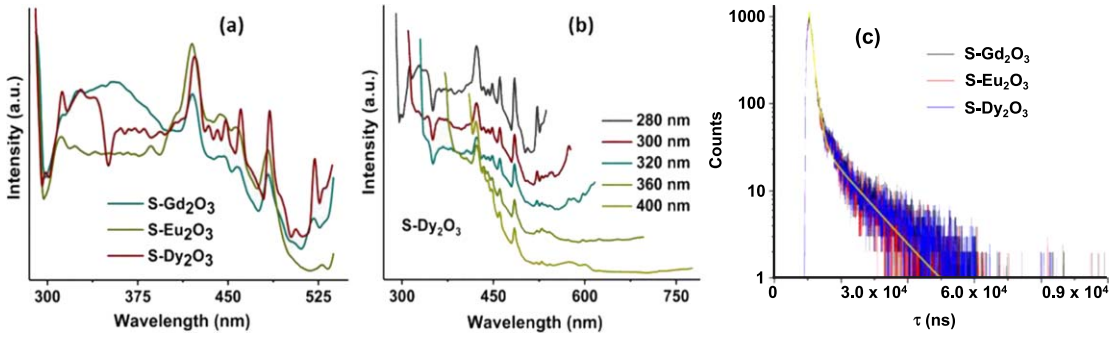

Figure 6. Photoluminescence spectra (a), of S-REO composites, emission spectra at different excitation wavelengths for S-Dy_2O_3 films (b) and decay profiles of the S-REO films ($\lambda_{ex} = 360$ nm) and $\lambda_{em} = 410$ nm).

Table 4. Values of lifetimes and their relative contributions for S-REO films.

Sample	τ_1, μs	τ_2, μs	a_1, %	a_2, %	χ^2
S-Gd_2O_3	1.10	9.47	70.77	29.23	0.99
S-Eu_2O_3	0.96	7.82	71.32	26.68	0.99
S-Dy_2O_3	1.08	10.12	73.44	26.56	0.996

The fluorescence decay measurements can reveal some details on the interaction nature between fluorophore and polymer matrix. The emission decay curves are given in figure 6(c) and the corresponding lifetime's values are reported in table 4.

The fluorescence decay profiles observed at 410 nm were satisfactorily fitted to a sum of two exponentials given by the following relation:

$$I(t) = a_1 \exp\left(\frac{-t}{\tau_1}\right) + a_2 \exp\left(\frac{-t}{\tau_2}\right) \quad (2)$$

where I(t) is the fluorescence intensity, τ_1, τ_2 represent the lifetimes and a_1, a_2 are the pre-exponential factors denoting the fractional contribution to time-resolved decay of the components with lifetimes τ_1 and τ_2, t is the time. This biexponential decay consists of a main component with a short lifetime around 1 μs and a contribution between 70.77 and 73.44% and a second component with a longer lifetime from 7.82 to 10.12 μs and the contributions vary between 26.56 and 29.23% (table 4). This biexponential behaviour with a shorter and longer lifetime could suggest that at least two coordination position of the rare metal oxide ion can occur in the polymer matrix. However the lifetime values obtained for S-REO composites are quite low as compared to reported values for Eu doped Y_2O_3 nanoparticles incorporated in a siloxane polymer ($\tau = 1.05$ ms) or Eu^{3+} doped siloxane networks (300–500 μs) [45, 46].

Knowing the moisture sorption in polymers is very important for a variety of industries ranging from microelectronics to adhesives and coatings [47]. For further applications in electronic devices, the elastomer should ensure a stable operation. This implies, among others, the stability of the characteristics of interest in different conditions of moisture and temperature [48]. To verify this, the moisture sorption-desorption isotherms were registered in dynamic regime (DVS) for the crosslinked composite films. Unlike the contact angle, which is a measure of the hydrophobicity of the surfaces, the DVS determine the moisture sorption capacity in the mass of the material. The water vapour sorption-desorption isotherms at room temperature recorded are shown in figure 7. The moisture sorption capacity values at 90% relative humidity (RH) are shown in table 5.

All samples show water sorption isotherms with a similar pattern: isotherms of III type characteristic for hydrophobic materials with hysteresis. The moisture sorption values estimated on their basis indicate that the known hydrophobicity of the silicone matrix (0.72 wt% in this case) is not affected by the incorporation of REOs, recording even a very slight increase of this in all three cases. Given that the values of the dipole moment (the measure of the electrical polarity of a system) for the three oxides increase in the order: $Eu_2O_3 < Gd_2O_3 < Dy_2O_3$ [49], it would be expected that the moisture sorption will increase in the same order, which it happens in the case of the first and the last. However, the values are very small, so the slight deviation of S-Gd_2O_3 from this hierarchy could be due to experimental errors (such as, for weighing).

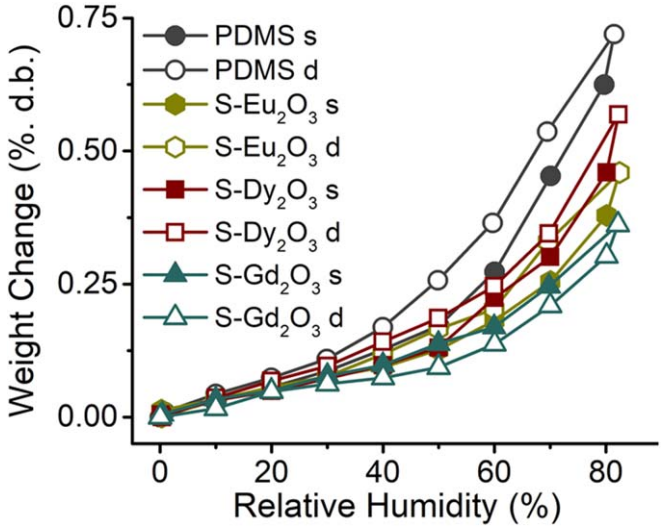

Figure 7. Water vapour sorption (s) -desorption (d) isotherms recorded on the prepared composites in the humidity range 0–90% RH. The humidity was increased in steps of 10%, the samples were maintained for 20 min at each humidity value.

Table 5. The moisture sorption capacity at 90% RH reached by the samples.

Sample	PDMS	S-Eu_2O_3	S-Gd_2O_3	S-Dy_2O_3
Weight gained (wt% d.b.[a]) -	0.72	0.46	0.39	0.57

[a] d.b.-dry basis.

3. Conclusions

The intrinsic hydrophobic nature of both the silicone used as the matrix and the rare metal oxides (in this case Eu_2O_3, Gd_2O_3 or Dy_2O_3) has made it possible to obtain highly dispersed composites of the latter without the need for prior compatibility treatments. The incorporation of rare earth oxides, in silicones leads to the modification of the studied properties, namely to increase the thermal stability, the dielectric permittivity, modulus and hydrophobicity. The fluorescence decay measurements reveal a biexponential behaviour with a shorter and longer lifetime suggesting that at least two coordination position of the rare metal oxide ion can take place in the polymer matrix.

Acknowledgments

This work was supported by a grant of the Romanian Ministry of Research and Innovation, CCCDI-UEFISCDI, project number PN-III-P1-1.2-PCCDI-2017-0185/76PCCDI/2018, within PNCDI III and European Cooperation in Science and Technology: COST Action CA15119. The author would like to thank Dr Ciobanu Constantin for his helpful advice on mechanical properties of composites examined in this paper.

ORCID iDs

Mihail Iacob https://orcid.org/0000-0002-3021-8903
Maria Cazacu https://orcid.org/0000-0003-4952-5548

References

[1] Wang L, Li B, Zhao X, Chen C and Cao J 2012 Effect of rare earth ions on the properties of composites composed of ethylene vinyl acetate copolymer and layered double hydroxides *PLoS One* 7e37781 (https://doi.org/10.1371/journal.pone.0037781)
[2] Mao X, Deng Y, Lin J and Chen Q 2014 Effects of rare earth samarium oxide on the properties of polypropylene- *graft* -cardanol grafted by reactive extrusion *J. Appl. Polym. Sci.* **131** 41012

[3] Burunkova J A, Denisiuk I Y, Zhuk D I, Daroczi L, Csik A, Csarnovics I and Kokenyesi S 2016 Fabrication and properties of luminescence polymer composites with erbium/ytterbium oxides and gold nanoparticles *Beilstein J. Nanotechnol.* **7** 630–6
[4] Sambhudevan S, Shankar B, Saritha A, Joseph K, Philip J and Saravanan T 2017 Development of x-ray protective garments from rare earth-modified natural rubber composites *J. Elastomers Plast.* **49** 527–44
[5] Nevyhoštěný S and Grégr J 2015 *Rare earth elements oxides nanoparticles for ionizing radiation Nanocon (Brno, Czech Republic)*
[6] Bezati F, Massardier V, Balcaen J and Froelich D 2011 A study on the dispersion, preparation, characterization and photo-degradation of polypropylene traced with rare earth oxides *Polym. Degrad. Stab.* **96** 51–9
[7] Xu F J and Qiu Z M 2010 Flame retardant composites of rare earth oxides/conventional flame retardants/ silicone rubber with good self-extinguishing *Adv. Mater. Res.* **152–153** 108–15
[8] Lane T H The Evolution of Silicones
[9] Kulyk K, Zettergren H, Gatchell M, Alexander J D, Borysenko M, Palianytsia B, Larsson M and Kulik T 2016 Dimethylsilanone generation from pyrolysis of polysiloxanes filled with nanosized silica and Ceria/Silica *Chem. Plus. Chem.* **81** 1003–13
[10] Mohammad Shiri H and Ehsani A 2016 A simple and innovative route to electrosynthesis of Eu_2O_3 nanoparticles and its nanocomposite with p-type conductive polymer: characterisation and electrochemical properties *J. Colloid Interface Sci.* **473** 126–31
[11] Uo M, Okamoto M, Watari F, Tani K, Morita M and Shintani A 2005 Rare earth oxide-containing fluorescent glass filler for composite resin *Dent. Mater. J.* **24** 49–52
[12] Majumder M, Choudhary R B, Thakur A K and Karbhal I 2017 Impact of rare-earth metal oxide (Eu2O3) on the electrochemical properties of a polypyrrole/CuO polymeric composite for supercapacitor applications *RSC Adv* **7** 20037-48
[13] Wang H, Zhang H, Su Y, Liu T, Yu H, Yang Y, Li X and Guo B 2015 Preparation and radiation shielding properties of Gd_2O_3/PEEK composites *Polym. Compos.* **36** 651–9
[14] Ren Q, Wan C, Zhang Y and Li J 2011 An investigation into synergistic effects of rare earth oxides on intumescent flame retardancy of polypropylene/poly (octylene-co-ethylene) blends *Polym. Adv. Technol.* **22** 1414–21
[15] Zhang H, Lu X and Zhang Y 2015 Synergistic effects of rare earth oxides on intumescent flame retardancy of Nylon 1010/ethylene-vinyl-acetate rubber thermoplastic elastomers *J. Polym. Res.* **22** 21
[16] Sarnecki J, Gawlik G, Lipińska L and Jeremiasz O 2015 Polymer luminescent concentrators containing oxide nanocrystals doped with rare-earth elements matched to an edge-illuminated silicon solar cell *Mater. Elektron. T.* **43** 10–17 nr **4**
[17] Liu Z, Li M, Hu Y, Fu H, Wang M and Jiang Z 2014 Dispersion and mechanical properties of cerium oxide filled into rubber composites *Rubber Chem. Technol.* **87** 340–7
[18] Sulym I, Goncharuk O, Sternik D, Terpilowski K, Derylo-Marczewska A, Borysenko M V and Gun'ko V M 2017 Nanooxide/Polymer composites with Silica@PDMS and Ceria–zirconia–Silica@PDMS: textural, morphological, and hydrophilic/hydrophobic features *Nanoscale Res. Lett.* **12** 152
[19] Kopylov V M, Kovyazin V A, Kostyleva E I, Fedorov A Y and Kovyazin A V 2016 The Thermal stabilisation and ceramifying of silicone rubbers *Int. Polym. Sci. Technol.* **43** 33–40
[20] Racles C, Musteata V E, Bele A, Dascalu M, Tugui C and Matricala A L 2015 Highly stretchable composites from PDMS and polyazomethine fine particles *RSC Adv.* **5** 102599–609
[21] Iacob M, Stiubianu G, Tugui C, Ursu L, Ignat M, Turta C and Cazacu M 2015 Goethite nanorods as a cheap and effective filler for siloxane nanocomposite elastomers *RSC Adv.* **5** 45439–45
[22] Iacob M, Tugui C, Tiron V, Bele A, Vlad S, Vasiliu T, Cazacu M, Vasiliu A-L A-L and Racles C 2017 Iron oxide nanoparticles as dielectric and piezoelectric enhancers for silicone elastomers *Smart Mater. Struct.* **26** 105046
[23] Quinsaat J E Q, Alexandru M, Nüesch F A, Hofmann H, Borgschulte A and Opris D M 2015 Highly stretchable dielectric elastomer composites containing high volume fractions of silver nanoparticles *J. Mater. Chem. A* **3** 14675–85
[24] Larmagnac A, Eggenberger S, Janossy H and Vörös J 2015 Stretchable electronics based on Ag-PDMS composites *Sci. Rep.* **4** 7254
[25] Nayak S, Chaki T K and Khastgir D 2014 Development of flexible piezoelectric Poly(dimethylsiloxane)–$BaTiO_3$ nanocomposites for electrical energy harvesting *Ind. Eng. Chem. Res.* **53** 14982–92
[26] Luo C, Hu S, Xia M, Li P, Hu J, Li G, Jiang H and Zhang W 2018 A flexible lead-free $BaTiO_3$/PDMS/C composite nanogenerator as a piezoelectric energy harvester *Energy Technol.* **6** 922–7
[27] Bele A, Tugui C, Sacarescu L, Iacob M, Stiubianu G, Dascalu M, Racles C and Cazacu M 2018 Ceramic nanotubes-based elastomer composites for applications in electromechanical transducers *Materials & Design* **141** 120–31
[28] Iacob M, Bele A, Patras X, Pasca S, Butnaru M, Alexandru M, Ovezea D and Cazacu M 2014 Preparation of electromechanically active silicone composites and some evaluations of their suitability for biomedical applications *Mater. Sci. Eng. C. Mater. Biol. Appl.* **43** 392–402
[29] Iacob M, Bele A, Airinei A and Cazacu M 2017 The effects of incorporating fluorinated polyhedral oligomeric silsesquioxane, [F3C (CH2)2SiO1.5]n on the properties of the silicones *Colloids Surfaces A Physicochem. Eng. Asp.* **522** 66–73
[30] Bele A, Dascalu M, Tugui C, Iacob M, Racles C, Sacarescu L and Cazacu M 2016 Dielectric silicone elastomers filled with *in situ* generated polar silsesquioxanes: preparation, characterization and evaluation of electromechanical performance *Mater. Des.* **106** 454–462
[31] Elliott P R, Stagon S P, Huang H, Furrer D U, Burlatsky S F and Filburn T P 2015 Combined hydrophobicity and mechanical durability through surface nanoengineering *Sci. Rep.* **5** 9260
[32] Cazacu M and Marcu M 1995 Silicone Rubbers. Ix. Contributions to Polydimethylsiloxane-α,ω-Diols Synthesis by Heterogeneous Catalysis *J. Macromol. Sci., Part A* **32** 1019–29
[33] Camino G, Lomakin S and Lazzari M 2001 Polydimethylsiloxane thermal degradation Part 1. Kinetic aspects *Polymer (Guildf).* **42** 2395–402
[34] Camino G, Lomakin S and Lageard M 2002 Thermal polydimethylsiloxane degradation. Part 2. The degradation mechanisms *Polymer (Guildf).* **43** 2011–5
[35] Johnson L M, Gao L, Shields C IV, Smith M, Efimenko K, Cushing K, Genzer J and López G P 2013 Elastomeric microparticles for acoustic mediated bioseparations *J. Nanobiotechnology* **11** 22
[36] Blythe A R, Blythe T and Bloor D 2005 *Electrical Properties of Polymers* (Cambridge: Cambridge University Press)
[37] Asandulesa M, Musteata V E, Bele A, Dascalu M, Bronnikov S and Racles C 2018 Molecular dynamics of polysiloxane polar-nonpolar co-networks and blends studied by dielectric relaxation spectroscopy *Polymer (Guildf).* **149** 73–84
[38] Pizzitutti F and Bruni F 2001 Electrode and interfacial polarization in broadband dielectric spectroscopy measurements *Rev. Sci. Instrum.* **72** 2502–4
[39] Samet M, Levchenko V, Boiteux G, Seytre G, Kallel A and Serghei A 2015 Electrode polarization vs. Maxwell-Wagner-Sillars interfacial polarization in dielectric spectra of materials: characteristic frequencies and scaling laws *J. Chem. Phys.* **142** 194703

[40] Ouyang G, Wang K and Chen X Y 2012 TiO_2 nanoparticles modified polydimethylsiloxane with fast response time and increased dielectric constant *J. Micromechanics Microengineering* **22** 074002
[41] Thomas H 1990 Courtney*Mechanical Behavior of Materials* (New York: McGraw-Hill)
[42] Wulff J, Wayne Hayden H and Moffatt W G 1965 *Structure and Properties of Materials* (New York: Wiley) vol 3
[43] Carpi F, Migliore A, Serra G and De Rossi D 2005 Helical dielectric elastomer actuators *Smart Mater. Struct.* **14** 1210–6
[44] Chauhan S, Kumar M, Chhoker S, Katyal S C and Awana V P S 2013 Structural, vibrational, optical and magnetic properties of sol–gel derived Nd doped ZnO nanoparticles *J. Mater. Sci., Mater. Electron.* **24** 5102–10
[45] Julián B, Corberán R, Cordoncillo E, Escribano P, Viana B and Sanchez C 2004 Synthesis and optical properties of Eu^{3+} -doped inorganic–organic hybrid materials based on siloxane networks *J. Mater. Chem.* **14** 3337–43
[46] Meltzer R S, Yen W M, Zheng H, Feofilov S P, Dejneka M J, Tissue B and Yuan H B 2001 Effect of the matrix on the radiative lifetimes of rare earth doped nanoparticles embedded in matrices *J. Lumin.* **94–95** 217–20
[47] Momen G and Farzaneh M 2011 Survey of micro/nano filler use to improve silicone rubber for outdoor insulators *Rev. Adv. Mater. Sci.* **27** 1–13
[48] Hanemann T, Gesswein H and Schumacher B 2011 Dielectric property improvement of polymer-nanosized strontium titanate-composites for applications in microelectronics *Microsyst. Technol.* **17** 1529–35
[49] Linton C, Chen J and Steimle T C 2008 Measurement of the electric dipole moments of cerium and praesodymium monoxides *OSU International Symposium on Molecular Spectroscopy* (OH, USA: Ohio State University)